COVER SHEET

Waclawik, E. R. and Bell, J. M. and Goh, R. G. and Motta, N. (2006) Investigations of self-organisation in composites of poly(3-hexylthiophene) on single-walled carbon nanotubes designed for use in photovoltaic applications. In Nicolau, Ian, Eds. Proceedings *SPIE "BioMEMS and Nanotechnology II"* 6036(8), pages 603607-1-603607-11, Brisbane.

Self-organization in composites of poly(3-hexylthiophene) and single-walled carbon nanotubes designed for use in photovoltaic applications.

Eric R. Waclawik[1]*, John M. Bell[2], Roland G. S. Goh[2], Anthony Musumeci[1], Nunzio Motta[2]

1. Inorganic Materials Research Program, School of Physical & Chemical Sciences, Queensland University of Technology, GPO Box 2434, Brisbane, AUSTRALIA, 4001
2. Centre for Built Environment and Engineering Research, Queensland University of Technology, GPO Box 2434, Brisbane, AUSTRALIA, 4001

ABSTRACT

A detailed study of poly(alkylthiophene) self-assembly and organization on single-walled carbon nanotubes (SWNTs) is presented. Experimental evidence for self-assembly and organization of regioregular poly(3-hexyl thiophene) (rrP3HT) on single-walled carbon nanotubes was obtained using scanning tunneling microscopy (STM) and transmission electron microscopy (TEM). TEM images of drop-cast rrP3HT/SWNT composites displayed strong evidence that SWNTs were isolated from each other in a polymer matrix and coated with between 1-3 layers rrP3HT. STM measurements of adsorbed monolayers of rrP3HT on SWNT surfaces were compared to rrP3HT monolayer deposition on highly ordered pyrolytic graphite (HOPG) surfaces. The results show that average inter-lamellar distances of adsorbed polymer are greater for rrP3HT monolayers adsorbed onto the curved surfaces of SWNTs than on the flat surfaces of HOPG samples. Analysis of STM images yielded the chiral angles at which the thiophene polymer chains wrap around individual carbon nanotubes (41-48º with respect to nanotube axis) while the interchain spacings of adsorbed macromolecules was 1.68 ± 0.02 nm. Comparisons between the native polymer deposited on graphite and the composite structure confirmed that the presence of carbon nanotubes in rrP3HT produces a material with a high degree of order at the molecular level. This high level of order and close coupling of the two components of the composite are prerequisites for its use as the active layer of an organic photovoltaic.

KEYWORDS

poly(3-hexylthiophene), single walled carbon nanotubes, polymer composites, scanning tunneling microscopy, self-assembly, molecular resolution, photovoltaics, organic electronics

1. INTRODUCTION

Conjugated polymer materials are of interest to scientists and engineers for a number of reasons, not least because they can be prepared with similar electrical and optical properties to semiconductors or even metals, while still retaining the attractive mechanical properties and processing advantages of polymers[1]. In the case of pure conjugated polymers, experimental studies have established direct correlations between electrical conductivity and mechanical properties of Young's modulus and tensile strength. That electrical properties and mechanical properties of conducting polymers improve together, in a correlated manner, as chain extension, chain alignment and inter-chain order are improved, reveals the important influence that intermolecular interactions, self-assembly and nanoscale structure have on such physical properties[1]. It is therefore not surprising that the properties of composites of conjugated polymers which have been formed by inclusion of either a second macromolecule or nanoscale inorganic within the material should be of interest to device scientists and engineers. New nanoscale polymer structures can form about the inserted materials leading to new and interesting physical properties. Polymer composite materials are used in a great variety of applications since they often possess superior mechanical properties such as increased tensile strength, elastic modulus and therefore flexibility, the area of fiber-reinforced composites is a long established field[2].

Recently interest in polymer composites has turned to their potential use in electronic applications, in so-called organic electronics. Not long after their discovery by MacDiarmid, Shirikawa and Heeger, conjugated or conductive polymer materials were quickly identified as promising candidates for use as the active component of a variety of electronic

BioMEMS and Nanotechnology II, edited by Dan V. Nicolau, Proc. of SPIE Vol. 6036, 603607, (2006)
1605-7422/06/$15 · doi: 10.1117/12.638665

devices, such as low-cost alternatives to conventional light-emitting diodes (LEDs), photovoltaic cells and even disposable electronic chips[3,4]. In the case of organic photovoltaics (OPVs), incorporation of a second material or dopant into the conjugated polymer to create a composite has led to great improvements in device performance compared to polymer-only devices[5, 6]. The organic semiconductor composite OPV active layer must be cast in the form of a bicontinuous network for it to operate as an efficient charge transport material, otherwise isolated domains will form which trap charge, leading to higher series resistances and thus low photocurrents[6]. Efficient charge transport therefore requires close packing of the second phase within the polymer. Since SWNTs have previously proven to be an effective electron transport component in OPVs[7], a structural study of a SWNT/conjugated polymer system is of interest since optical and electrical properties of conjugated polymer composites strongly depend upon polymer nanoscale structural organization.

1.1 Bulk heterojunction diodes

The device architecture of early OPVs closely mimicked inorganic heterojunction devices, they consisted of a bilayer of p-type and n-type organic semiconducting polymers sandwiched between two metal contacts. Charge separation of excitons photogenerated near the p-n junction interface ultimately led to a photocurrent. Unfortunately the sunlight-to-electrical conversion efficiency of bilayer OPVs were disappointingly low. The reasons for this were twofold. Unlike inorganic semiconductor devices which are doped with heteroatoms to produce majority and minority carriers, organic semiconductors are either intrinsically p-, or n-type. Because they are not doped, no internal field develops at the heterojunction, the requirement of an internal electric field thus requires metals (often oxygen-sensitive metals) possessing different workfunction to be deposited either side of the bilayer device[6]. The second and more important difference is that the *molecular nature* of the organic semiconductor leads to a HOMO/LUMO picture of electronic energy levels rather than extended valence and conduction bands. Excitons are strongly coupled to the molecular geometry of the polymer and possess a strong Coulomb interaction or exciton binding energy. Organic excitons are thus Frenkel excitons, the size of which rarely extend further than approximately three polymer repeat units (~10 nm typically), the diffusion radius of these excitons is quite short (~5 nm)[8]. A direct consequence of the short exciton diffusion radius is that only excitons generated within a few nanometers of the polymer bilayer interface have a high probability of being separated into carriers in these OPVs. The external quantum efficiencies (EQEs) of these devices are thus severely limited[9].

The ability to process conjugated polymers from solution provides a way to overcome the problem of short exciton diffusion length. An electron donor can be combined with an electron acceptor to create a composite material which can operate as the OPV active layer. This distributed p-n junction approach to organic photovoltaic device engineering has been called the bulk heterojunction approach[6]. Blends of different polymers are processed a particular solvent which are then combined and spin cast onto a substrate to create an interpenetrating polymer network. By arresting phase phase-separation at an early stage such all-polymer composite OPVs form a bicontinuous network (at the nanoscale) throughout which exciton generation and charge separation can occur. High EQE OPVs can be constructed from these materials provided both components are percolated, meaning that there is a conductive path between the metal terminals that photogenerated electron and hole charge carriers can traverse[10].

Another approach to creating a heterojunction OPV is to cast a semiconducting polymer layer containing an inorganic material. A number of different polymer/inorganic material combinations have been investigated as heterojunction OPVs[4]. Derivatives of polyaniline, polyphenylene vinylene and polythiophene which have been doped with small amounts of inorganic materials such as CdSe or fullerene are three well known examples which have been explored in this context[11,5]. To date the most efficient such bulk heterojunction OPVs have been formed from poly((2-methoxy-5-(2'-ethylhexoxy)-*p*-phenylene) vinylene) (MEH-PPV) and soluble fullerene derivatives[10]. Optimum performance in these devices occurs at high fullerene loads (80%), which indicates that percolation is easier to achieve in the polymeric component than the non-polymeric component. Quantum efficiencies approaching 3% have been reported[9].

1.2 Factors affecting external quantum efficiency in bulk heterojunction OPVs

Organic conjugated polymers are not completely crystalline, spin cast films contain both crystalline and amorphous regions. This can clearly be observed using x-ray diffraction, where the spectrum of these partially crystalline polymers display sharp peaks due to crystalline scattering superimposed over a broad background assigned to amorphous

scattering[12]. Since defect-free, crystalline conjugated polymers have the higher charge transport mobility, maximizing effective polymer crystallinity is of paramount importance in OPV device applications. Film morphology and the ratio of crystalline to amorphous polymer strongly depend on spin casting conditions (eg. speed, temperature) and the choice of solvent used to cast films. Annealing of films just below the glass transition temperature of the polymer can "iron-out" defects in individual polymer chains which has a beneficial effect when trying to increase polymer crystallinity[13]. In the case of organic conjugated polymer composites, there is a second effect which can influence polymer crystal structure and that is the interactions between the dopant and polymer. If there is large mismatch between the polymer's preferred crystal lattice structure and the crystal structure of the dopant material, the second phase can be a source of defects in polymer nanostructure. Where this occurs, high loadings of the non-polymeric component within the composite may reduce the conjugated polymer's overall crystallinity and thereby decrease charge carrier mobility within the composite material. A high weight percent of the non-polymeric component within the composite can also affect charge carrier mobility in other ways. Aggregation of the second phase can occur at high dopant concentrations when spin cast from solution[13]. It is thus quickly apparent that competing factors must be considered when designing organic semiconductor composites for use in bulk heterojunction OPVs. High loadings of the non-polymer component are needed to assure percolation of charge through the bicontinuous network, however the loadings must be low enough such that neither isolated aggregates of one component form, nor breakdown in polymer crystalline order occurs either.

Third, in order to obtain good EQE from a bulk heterojunction OPV, good overlap between the absorption spectrum of the conjugated polymer and the solar spectrum is desirable. The optical bandgap of a typical organic semiconducting polymer such as poly(phenylenevinylene or poly(3-hexylthiophene) occurs in the range 600 to 300 nm, where the electronic excitation is often coupled to a vibrational mode in the polymer[14]. The wavelength range over which light absorption by conjugated polymers occurs depends on the amount of conformational disorder of individual polymer chains within the cast films. A conjugated polymer can be considered to consist of a string of *effectively conjugated segments* (ECS) over which the polymer's π-electron cloud maintains coherence. At the end of each effectively conjugated segment, one photophysical unit ends and another begins. The length of effective conjugated segments in a conjugated polymer can often be limited by conformational disorder, although this not the only limiting factor. Entropy considerations mean that for large molecular weight polymers no individual polymer main-chain can have a perfectly ordered backbone, there will be some degree of conformational disorder (eg. chain-twists or polymer chain hairpin folds). Consequently, absorption spectra are a superposition of the spectra of ECSs of slightly different lengths. This causes inhomogeneous broadening of vibronic bands, increasing overlap with the solar spectrum[6].

1.3 Poly(3-hexylthiophene)/single walled carbon nanotube composites for bulk heterojunction diodes

The electrical and optical properties of composites formed between carbon nanotubes and poly-(alkylthiophenes) makes them very promising candidates for use in organic photovoltaic devices[15]. Both materials can be readily dispersed in common organic solvents suitable for spin casting the composite films[7]. Most conjugated polymers are very insoluble in common solvents. This is because a rigid polymer backbone is often the requirement to maintain significant π-electron delocalization along the chain. However an insoluble conjugated polymer such as polythiophene can be granted solubility by grafting flexible side chains to the main polymer backbone. This increases the entropy of solution and entropy of melting of the material making it soluble and tractable but without losing main-chain conjugation. The solubility requirement for side-chain decoration on the polymer can have a profound effect on polymer crystalline structure, optical and electrical properties, depending on the nature of the side-chain and its position of attachment. This is clearly demonstrated in the case of poly(3-hexylthiophene) by comparing the charge transport mobility of the regioregular form of P3HT (rrP3HT mobility = 0.1 cm^2/Vs) with regiorandom P3HT of the same average molecular weight (rraP3HT mobility = 10^{-7} – 10^{-4} cm^2/Vs cm^2/Vs)[16]. The only difference between these two forms of the same material is that the former possesses a hexyl side-chain attachment on the 3-position of the thiophene ring while the latter contains hexyl side chains randomly attached at either the 3 or 5 position of the thiophene units of the polymer. When cast into a film, the regioregular P3HT is more likely to form an ordered, head-to-tail coupled solid, with fewer amorphous regions compared to the regiorandom form[16]. P3HT is a semi-crystalline polymer and in the crystalline region is believed to conduct current through both inter and intra-chain transport, whereas in the amorphous region, transport is through hopping or tunneling processes only[13]. The significant influence of non-covalent, intermolecular interactions within the polymer upon electrical charge transport is clearly demonstrated by this comparison.

If changes in molecular order strongly affect P3HT film conductivity, rrP3HT structures formed at P3HT/SWNT interfaces throughout the composite are likely to be important in determining the overall efficiency of heterojunction OPVs made from this material. In a comparable composite system Blau and co-workers have studied the wrapping of carbon nanotubes (CNTs) with a variety of conjugated polymers including poly(*m*-phenylenevinylene-*co*-2,5-dioctyloxy-*p*-phenylene vinylene) (PmPV) and have demonstrated that inclusion of nanotubes in PmPV forms composite materials with enhanced electrical conductivity and mechanical strength[17, 18]. Importantly, they also recently demonstrated that nanotubes nucleate polymer crystallinity[17]. Recently, Bai and coworkers imaged the ordering and molecular folding of PmPV absorbed onto HOPG and suggested that the observed molecular ordering and folding relates directly to the wrapping of PmPV on CNTs in PmPV/CNT composite materials[19]. They proposed that a planar conformation favoured strong overlap between the π-orbitals of the graphite and π-electrons of the conjugated polymer which also is expected to be adopted during the wrapping of PmPV on CNTs in PmPV/CNT composite materials. The main purpose of this work was to study the wrapping of the highly conductive and crystalline conjugated polymer poly(3-hexylthiophene) in its regioregular form on single-walled carbon nanotubes to clarify the polymer organization and aggregation of polymer at SWNT interfaces and in the bulk of the composite. A likely requirement for efficient electron-injection from rrP3HT to carbon nanotubes in an OPV constructed from this composite material is close physical contact of the P3HT, preferably in some crystalline or ordered monolayer form at the SWNT interfaces throughout composite film. A further motivation for this investigation relates to an ultimate use for rrP3HT-wrapped SWNTs in future nanotechnology applications. We note that carbon nanotubes are formed from the same material as graphite (*ie*. SWNTs can be considered as a seamless rolled-up sheet of graphene)[20], information on polymer structures that form at the carbon nanotube interfaces can thus be directly compared to structures formed from rrP3HT films drop cast onto highly ordered pyrolytic graphite to determine the importance of substrate curvature on polymer wrapping.

2. EXPERIMENT

AP (as-prepared) grade SWNT with a quoted purity of around 70% obtained from Carbolex Inc. was purified using a modification of the method of Smalley and co-workers[21]. Briefly, the nanotubes were refluxed for 40 hours in 2.6M HNO_3 and filtered through 75nm pore size Anodisc membranes. Cutting was performed by sonicating the purified tubes in a 2:1 HNO_3/H_2SO_4 mixture for 2 hours and subsequently polished by stirring in 4:1 H_2O_2/ H_2SO_4 at 70°C. The tubes were washed with copious amounts of de-ionized water (18.2MΩ) and characterized using SEM and Raman spectroscopy to confirm efficacy of treatment procedure. Fourier Transform Raman spectra were collected on a Perkin-Elmer System 2000 FT-Raman operating at 1064 nm with 4 cm^{-1} resolution[22].

Regioregular P3HT (98% head-to-tail coupling) was obtained from Sigma-Aldrich company and used without further purification. rrP3HT solutions (4mg/ml) consisting of 5% by weight of purified-SWNTs were prepared by mixing in chloroform in an ultrasonic bath for at least 1 hour following the procedure of McCarthy *et al*. to promote polymer/nanotube interaction[23]. For STM experiments, films were prepared by casting a drop of the supernatant solution onto surface of freshly peeled HOPG (highly oriented pyrolytic graphite – ZYA grade, obtained from NT-MDT). The drop was observed to dry within seconds. STM measurements were conducted on an NT-MDT Solver SPM apparatus. Tunnelling conditions, optimized for individual drop-cast samples and over time, are reported in captions accompanying the images. Tip quality was checked by obtaining atomic resolution of the graphite substrate before every film deposition. Images presented are unfiltered unless indicated otherwise. TEM imaging was performed in a Philips 200 STEM. To prepare samples for TEM imaging a dilute solution of the SWNT/rrP3HT composite in chloroform was drop-cast onto holey carbon grids and allowed to dry in air.

3. RESULTS

3.1 Transmission Electron Microscopy of rrP3HT/SWNT Composites

TEM images of individually-wrapped single-walled carbon nanotubes are presented in Figure 1. From inspection of Figure 1 it is clear that the SWNTs were coated with a thin (5 nm) layer of the polymer. In all images a central hollow core with width commensurate with the nanotube diameters as determined by Raman spectroscopy (~1.4nm) can be clearly observed. Analysis of several similar TEM images of rrP3HT-coated nanotubes (*eg*. Figure 1b) revealed that the polymer coated individual some SWNTs to a thickness of 20 nm in some cases. These TEM images indicate that the SWNT purification and dispersion technique employed leads to a composite formed from *individually polymer-wrapped*

SWNTs rather than P3HT-wrapped nanotube aggregates, or ropes. Spin-cast films of these composites are therefore also likely to consist of individually rrP3HT-wrapped SWNTs. This being the case, fibers imaged in STM were expected to be coated to a minimum thickness of between 1-3 polymer layers.

In studies of a similar composite system, TEM investigations of polymer coating thickness in the case of PmPV composites with SWNTs revealed that coated SWNTs formed intertwined ropes with fiber diameters in the range 70-120 nm each containing of 20-80 SWNTs[18]. This could explain differences in STM measurements observed here for rrP3HT/SWNT composite system and PmPV/SWNT composites where only thickly-coated SWNTs could be identified and without molecular resolution. A large number of polymer dendrimer growths were observed by these authors, particularly near the tips of polymer-coated carbon nanotubes. Since carbon nanotubes contain more defects at their tips, it was concluded that the dendritic polymer growths were nucleated at these defects[18]. No such polymer growths were observed here in the case of TEM images of rrP3HT-wrapped SWNTs which may indicate the SWNTs used possessed fewer defects, although differences arising due to the solvent system employed and the different polymer molecular structure cannot be ruled out.

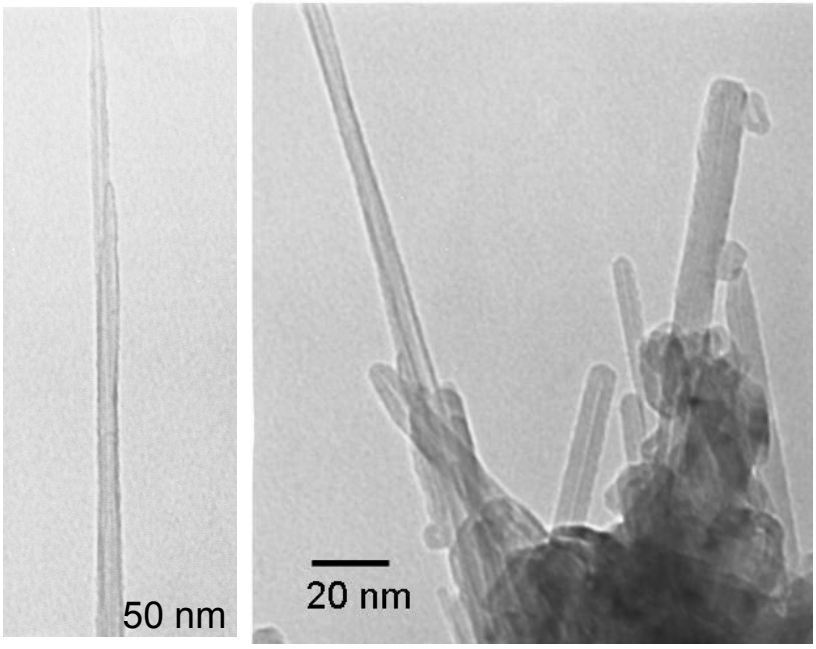

Figure 1. (a) TEM image of two rrP3HT-wrapped SWNTs drop-cast from chloroform solution. The polymer coating is approximately 5 nm thick. From analysis of Raman spectrum the diameters of nanotubes are approximately 1.4 nm. (b) TEM image of several SWNTs coated with polymer layers of thickness between the range of 5-10 nm.

3.2 Scanning Tunneling Microscopy of rrP3HT films on HOPG

Since a SWNT can be considered as a seamless rolled-up sheet of graphene, a comparison between STM measurements of P3HT/SWNT composites and P3HT-coatings on HOPG might be used to determine the importance of simple geometric factors such as the graphene surface curvature in P3HT ordering at sp^2-bonded carbon interfaces in composites. Hence, we firstly performed STM investigations of rrP3HT films cast from chloroform solutions onto HOPG. We investigated drop-cast films of rrP3HT solutions with low (~1μg/ml) and high (~4mg/ml) polymer concentration, the latter being a concentration equivalent to those used for the rrP3HT/SWNT composites. The large electron density of the conjugated backbone of rrP3HT was expected to appear as bright features in STM images as the only component of the conjugated polymer imaged based on previous studies[19]. Figure 2a shows a rrP3HT monolayer film cast from a diluted solution of chloroform where the bright domains attributed to the conjugated backbone of polymer chains are clearly aligned in rows on the HOPG surface. Based on the approximate 0.2 nm height and 1.2 nm width of the bright domains measured in the linescan of Figure 2a, our hypothesis as to the origin of the bright domains was confirmed. The measured height and width is consistent with planar adsorption of the conjugated backbone of rrP3HT onto HOPG, an orientation which is expected maximize the overlap of the π-electron system of rrP3HT with the highly delocalized electron system of graphite. Additionally, the measured chain to chain distance is 1.45 nm, this is within the range measured for this system by Mena-Osteritz *et al*[24]. The presence of 60º and 120º folds is evidenced by the dark blue lines overlaid on the image.

The STM images of P3HT thick coating (Figures 2b-2c) on graphite appear as a fairly uniform film at the microscale. Most of the surface is covered by a thick layer, but in some areas we were able to resolve the underlying flat-lying surface polymer layer. Linear strands and folded chains could clearly be observed (boxed region of Figure 2b) in these areas, suggesting 2D ordered assembly in the adlayer just below the thick P3HT aggregates.

However because of the thick coating, most of the surface is covered by bright islands approximately 2nm higher than the folded chains (Figure 2b) which is also visible in our images. This could correspond to approximately one lamellar layer sitting on top of the background layer with π-stacking normal to the substrate ,as found when the polymer is deposited by repetitive dip-coating via Langumuir Blodgett technique[25, 26]. The total layer thickness is about 4 nm as apparent from Fig 1c. The STM results displayed in Figure 1 are thus a confirmation of the Stranski-Krastanov type of mechanism that previously been proposed for the formation of these films. That is; a well ordered primary layer deposits at the HOPG surface, followed by subsequent formation of 3-dimensional islands of P3HT.

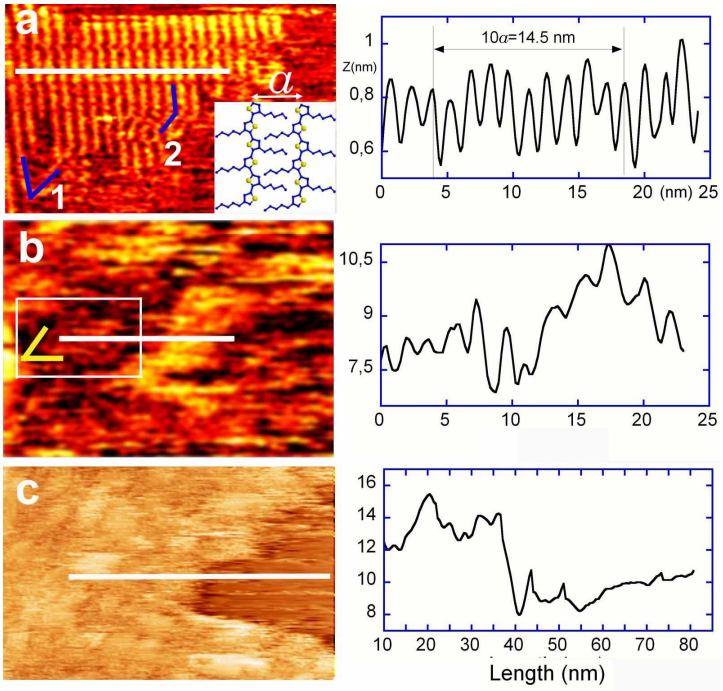

Figure 2. Right: series of STM images of drop cast P3HT film on HOPG. Left: line profile to show the film surface structure.
a) Monolayer P3HT film showing the interdigitated P3HT structure. 1 and 2 are 60° and 120° folding chains respectively. *Inset*: drawing of the interdigitated structure showing *a*, the chain-chain distance. From the line profile (left) a=1.45 nm.
b) Thick polymer layer showing chains and fold of polymer chains appearing on the left of a thick island. V_{bias} =0.103V; I= 0.098nA. Line profile of the transition shows that the island sits approximately 2nm above the bottom layer.
c) Thick P3HT coating showing a bare surface region. V_{bias} =0.58V; I= 0.07nA. The measured thickness of the coating from line profile is about 4 nm.

3.2 Scanning Tunneling Microscopy of rrP3HT/SWNT Composites

Figure 3 shows P3HT/SWNT composites imaged at various length-scales using STM. The high aspect ratio of the SWNTs allowed them to be easily located, even when covered with rrP3HT polymer. It is immediately apparent from Figure 3a that there was an abundance of rod-shaped features throughout the composite which we interpret as being SWNTs are obscured by thick polymer coatings. In Figure 3b a SWNT with ends pinned by polymer islands is visible, along with a short tube of about 30nm lying adjacent to it. A magnified view of the shorter tube is shown in Figure 3c, where it can be seen that the polymer coats the tube evenly over its length. The diameters of the carbon nanotubes used in this study was ~1.4nm as determined from Raman spectroscopy[27]. With the π-π stacking distance of polymer being estimated to be 0.38nm, and taking into consideration the van der Waals radius, a monolayer-wrapped tube should be 2.16 nm thick[28]. Measured tube heights vary between 2.1 and 2.5 nm, matching the expected value for the diameter if we include the nanotube-substrate distance of 0.25 nm; hence we believe these objects to be individual single-walled carbon nanotubes coated with one layer of polymer. The rod-shaped features are thus likely to be rrP3HT-coated SWNTs with lengths ranging from tens of nanometers to about 200 nanometers.

A high a degree of rrP3HT polymer chain organization, *i.e.* polymer wrapping, can be seen along the entire tube axis. This confirms the view that when ultrasonically-dispersed in a polymer solution, the carbon nanotubes absorb as many strands of polymer as possible to reduce interactions with adjacent tubes[28]. The cross section measurement along the axis reveals a periodicity of approximately 1.66 nm. Measurements of several tubes yielded an average chain-to-chain distance of 1.68 ± 0.02 nm. This is significantly larger than rrP3HT monolayer polymer chain-to-chain distances (d_{cc}) measured on HOPG by both Grevin *et al* and Mena-Osteritz *et al*[24, 29]. These studies yielded values of $d_{cc} \approx 1.4$ nm and $d_{cc} \approx 1.33$ nm respectively for this system. In the case of rrP3HT adsorbed onto HOPG (Figure 2a) we measured $d_{cc} \approx 1.45$ nm, in accordance with earlier studies[24, 29] and may therefore be confident that the larger d_{cc} for rrP3HT monolayers on SWNTs is a true value and not some instrumental artifact.

In addition to an average measurement of $d_{cc} = 1.68 \pm 0.02$ nm, we were also able to extract the chiral angle of polymer wrapping measured with respect to the nanotube long-axis from the STM scans (Figure 4) where individual rrP3HT thiophene chains are resolved. The value measured here is 48º(±4º), while in Figure 3 we measured a wrapping chiral angle of 41º(±4º). Polymers have usually been observed to wrap the tubes with a chiral angle with respect to the tube axis, suggesting a connection between the macromolecular coiling process to the underlying chirality of the tube[30]. The different measured interchain distances and chiral angles observed for individual rrP3HT-coated nanotubes suggest that at least for the case of rrP3HT composites, carbon nanotube chirality could significantly influence the polymer structures depositing at the surface. This does not however rule out other possible macromolecule alignments and arrangements (such as lengthways) along the carbon nanotubes. Electronic effects may very well be predominant in the interactions of polymers with the small diameter single-wall carbon nanotubes.

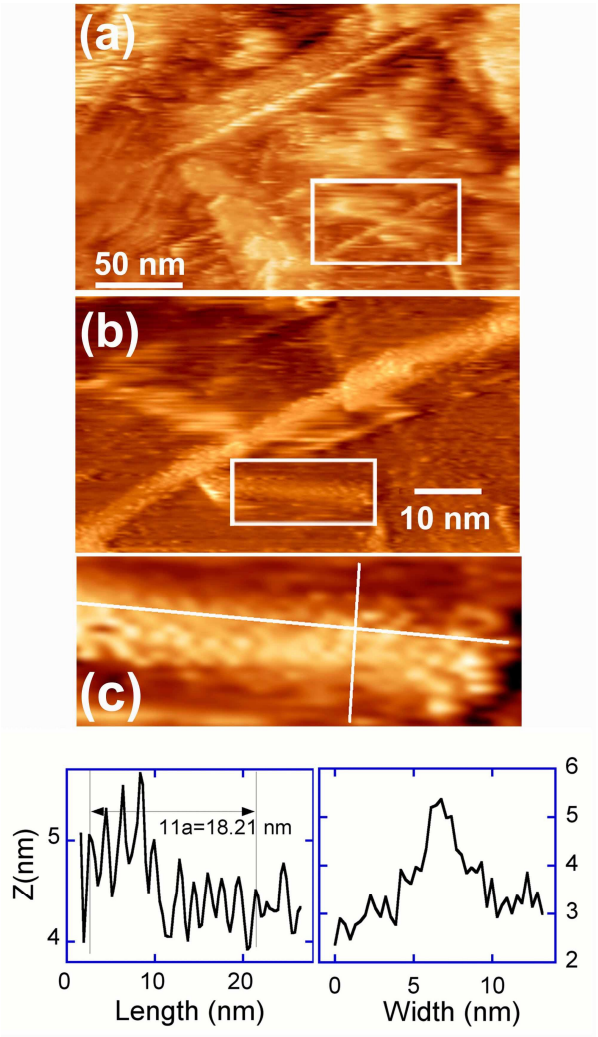

Figure 3. (a) STM image of cast film shows an abundance of nanotubes dispersed throughout the polymer matrix; V_{bias} = 0.512V; I = 0.053nA. (b) A zoom of this nanotube reveals an ordered pattern on the tube body, a short tube of about 30nm is also revealed at this high resolution zoom; V_{bias} = 0.661V; I= 0.093nA . (c) Zoom of the short nanotube in (b) with cross sections: the repeat distance along the SWNT long-axis is 1.66 nm; the measured height is 2.5 nm, corresponding to the tube diameter plus the polymer thickness.

4. DISCUSSION

To date, STM studies of conducting polymers which have revealed details of polymer-monolayer chain folding and self assembly have been performed by drop-casting films from dilute solutions onto HOPG[19, 24, 29]. However, polymer composite films used in organic electronic devices are typically cast from more concentrated solutions (on the order of 1 mg/ml or greater) where bulk effects are likely to be affecting their organization and assembly[25]. From analysis of STM results in Figure 2, we have seen evidence for the Stranski-Krastanov type of film growth that occurs when films of rrP3HT are drop-cast from concentrated P3HT solutions onto HOPG. The films produced from concentrated P3HT solutions appear to possess regions where deposition is thicker than the average thickness of the film as measured by STM. These regions are readily observed in Figure 2c and are typically 10-20 nm in width, while STM cannot provide information on crystallinity (STM provides only electronic and topographical information), it is possible that these domains in the film correspond to crystalline grains of polymer which have accumulated at the surface of the initial P3HT monolayer during the drop-casting process. This value for a typical rrP3HT aggregation differs significantly from

the size obtained by Sandberg *et al* using atomic force microscopy measurements on thin rrP3HT films which gave aggregate sizes of between 50-100 nm[25]. This difference indicates just how sensitive film formation is to casting conditions. While our films were cast in one step from a concentrated solution of P3HT in chloroform, Sandberg *et al* built-up their films by repetitive dip-coating from a dilute solution of P3HT in xylene. The degree of polymer aggregation in solution is a strong function of polymer concentration, polymer solubility and solution temperature. These aggregated states become "frozen-out" or are maintained when spin-cast films are deposited from these solutions[31]. Based on a comparison of these results, it is likely that solutions cast from xylene will produce larger rrP3HT aggregates and therefore possibly larger crystalline domains possessing high charge mobility.

A comparison of the rrP3HT structures formed at a flat HOPG interface compared to a curved SWNT interface is instructive. Our measurements of rrP3HT monodomains on HOPG yielded an average polycrystalline area of ≈ 40 nm (⊥ to P3HT π-conjugated backone) x 20 nm (// to P3HT π-conjugated backone). This size is approximately the same order as the typical coherence lengths reported from XRD measurements[29].On a more local scale, analysis of STM images showed that adsorbed polymer chain-to-chain distances correspond to a densely packed 2D-monolayer where interaction with the HOPG surface promotes full interdigitation of the P3HT side-chains (d_{cc} = 1.45 nm). This chain-to-chain distance is smaller than the equilibrium value obtained in thin films studied by XRD (d_{cc} = 1.6 nm)[25]. It appears that the XRD result for bulk rrP3HT films yields an inter-lamellar spacing similar to the inter-chain distance measured for rrP3HT monolayers on SWNTs. One factor that may lead to this increase in d_{cc} of rrP3HT monolayers on a curved surface is the differences in the size of the underlying hexagonal structure of HOPG compared to SWNT. While both forms of carbon consist of the same material, the curvature of the graphene surface to form a typical single-walled carbon nanotube leads to a largercarbon-carbon bond distance, $a_{c\text{-}c}$ = 1.44 Å compared to $a_{c\text{-}c}$ = 1.42 Å for HOPG[20]. In STM studies of straight-chain alkane hydrocarbons adsorption onto HOPG it has been noted that good lattice match between the hydrocarbon backbone and the graphite lattice favours commensurate packing of the hydrocarbon film with the underlying substrate[32]. The hexyl side chains (and the polythiophene polymer backbone) of the adsorbed rrP3HT is thus likely to experience a different interaction with the HOPG surface compared to a SWNT surface which could lead to the differences in packing observed. At the local scale epitaxial effects are believed to promote the full interdigitation of P3HT hexyl side-chains to give the energetically most stable state on HOPG, this results in a dense packing of macromolecules. The disparity between rrP3HT adsorbed onto HOPG and onto SWNTs may thus indicate that the substrate curvature plays a fundamental role in assembly of ordered domains. The importance of the role of substrate curvature was recently demonstrated in dramatic STM images of monolayer protected nanoparticle surfaces, this underlies the importance that factors such as geometrical constraints and surface stress anisotropy may have upon monolayer deposition[33].

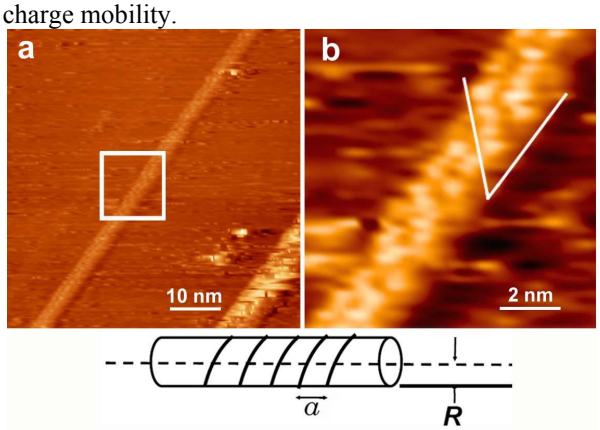

Figure 4. a) STM image of a rrP3HT-coated SWNT. (b) Zoom-in of the boxed area. The chiral angle of the polymer wrapping with respect to the nanotube long-axis is 48º as indicated in (b). STM settings: V_{bias} = 0.271V; I= 0.102nA. The direction of polymer wrapping is indicated in the schematic.

The way in which polymers adsorb onto carbon nanotubes has been investigated by various authors, leading to two contradictory conclusions: based on their STM measurements of PmPV monolayers on HOPG, Lei *et al*[19] suggested that the conjugated polymer's self-assembly and arrangement is dominated by the matching of the graphene structure with the detailed structure of the conjugated polymer, and that the same intermolecular forces are likely to induce self-assembly when PmPV is adsorbed onto carbon naotubes. However, Coleman *et al* [34] have pointed out that geometric factors and constraints imposed by a narrow crylindrical structure, like a SWNT on a conjugated polymer chain, may outweigh any lattice-resolved contributions (*eg*. carbon nanotube chirality) to polymer ordering. Specifically the elastic energy cost of bending the conjugated polymer backbone so as to maintain close contact between macromolecule and nanotube surface can energetically favour certain polymer coiling-angles. Differently sized carbon nanotubes will favour a different chirality of polymer coiling. In this model, the periodic potential of the hexagonal lattice[35] is also expected to play an important role in the geometrical arrangement of P3HT on the nanotube surface .For the case of SWNT wrapping by PmPV, Coleman *et al*'s[34] recently formulated model works well due to the fact that PmPV is a "stiffer" polymer

compared to P3HT (10nm persistence length[34] compared to 2.1nm for P3HT[36]). In fact by applying the same model to polyacetylene (1.3nm persistence length), the authors found no preferential coiling angle for the less stiff polymer; the periodic potential of the hexagonal lattice[35] is thus expected to play an important role in the macromolecule's coiling angle and geometrical arrangement in the case of templating of rrP3HT on SWNTs.

5. CONCLUSIONS

In summary, we have imaged by STM the arrangement of rrP3HT on HOPG and nanotubes. While 2D crystals are observed when rrP3HT is cast onto HOPG from dilute solution, we have found a thicker and more disordered film when cast from our concentrated solutions. The subsequent layers are more likely to align normal to underlying monolayer on HOPG[37]. rrP3HT monolayers have the tendency to wrap around SWNTs, where thiophene and hexyl moieties associate with the SWNT surface in identical manner to rrP3HT monolayer depositions on HOPG. We have performed measurements of the chain to chain distance, finding an average value on SWNTs (1.68 nm) 20% larger than on HOPG. It is likely that the measured differences of interchain-spacing of rrP3HT monolayers on SWNTs and on HOPG arise because of substrate curvature.

6. ACKNOWLEDGEMENTS

The authors acknowledge financial support from both the QUT Strategic Collaborative Grant for Applied Nanotechnology and the Inorganic Materials Research Program. R.G. acknowledges the QLD Government for a Smart State Award in support of this work.

7. REFERENCES

(1) Heeger, A. J. In *Conjugated Polymers and Related Materials. The Interconnection of Chemical and Electronic Structure.*, Proceedings of the Eighty-first Nobel Symposium., Luleå, Sweden, June 13-18, 1991; Salaneck, W. R.; Lundström, I.; Rånby, B., Eds. Oxford University Press, 1993; pp 27 - 62.

(2) Dalton, A. B.; Collins, S.; Munoz, E.; Razal, J. M.; Ebron, V. H.; Ferraris, J. P.; Coleman, J. N.; Kim, B. G.; Baughman, R. H., *"Super-tough carbon-nanotube fibres - These extraordinary composite fibres can be woven into electronic textiles"*, Nature (London), **423**, 703-703, 2003**.**

(3) Shirakawa, H.; Louis, E. J.; MacDiarmid, A. G.; Chiang, C. H.; Heeger, A. J., J. Chem. Soc., Chem. Commun, 578, 1977**.**

(4) Star, A.; Lu, Y.; Bradley, K.; Gruner, G., *"Nanotube optoelectronic memory devices"*, Nano Lett., **4**, 1587-1591, 2004**.**

(5) Spanggaard, H.; Krebs, F., C., *"A brief history of the development of organic and polymeric photovoltaics"*, Solar Energy Materials & Solar Cells, **83**, 125-146, 2004**.**

(6) Grell, M., Chapter 6: Electronic and electro-optic molecular materials and devices. In *Nanoscale Science and Technology*, Kelsall, R., W.; Hamley, I., W.; Geoghegan, M., Eds. John Wiley & Sons: Chichester, 2005; pp 282-342.

(7) Kymakis, E.; Alexandrou, I.; Amaratunga, G. A. J., *"High open-circuit voltage photovoltaic devices from carbon-nanotube-polymer composites"*, Journal of Applied Physics, **93**, 1764-1768, 2003**.**

(8) Gregg, B., A., *"Excitonic Solar Cells"*, J. Phys. Chem. B., **107**, 4688-4698, 2003**.**

(9) Brabec, C., J., *"Organic photovoltaics: technology and market"*, Solar Energy Materials & Solar Cells, **83**, 273-292, 2004**.**

(10) Brabec, C., J.; Saiciftci, N. S.; Hummelen, J., C., *"Plastic Solar Cells"*, Adv. Func. Mater., **11**, 15-26, 2001**.**

(11) Huynh, W. U.; Dittmer, J. J.; Alivisatos, A. P., *"Hybrid nanorod-polymer solar cells"*, Science, **295**, 2425-2427, 2002**.**

(12) Samuelsen, E. J.; Mårdalen, J., In *Handbook of Organic Conductive Molecules and Polymers*, Nalwa, H. S., Ed. 1997; Vol. 3, pp 87-120.

(13) Schwartz, B. J., *"CONJUGATED POLYMERS AS MOLECULAR MATERIALS: How Chain Conformation and Film Morphology Influence Energy Transfer and Interchain Interactions"*, Ann. Rev. Phys. Chem., **54**, 141-172, 2003**.**

(14) Ruhe, J.; Colaneri, N. F.; Bradley, D. D. C.; Friend, R., H.; Wegner, G., *"Photoexcited states in poly(3-alkyl thieneylenes)"*, J. Phys.: Condens. Matter, **2**, 5465-5476, 1990**.**

(15) Kymakis, E.; Alexandou, I.; Amaratunga, G. A. J., *"Single-walled carbon nanotube-polymer composites: electrical, optical and structural investigation"*, Synth. Met., **127**, 59-62, 2002**.**
(16) Sirringhaus, H.; Brown, P. J.; Friend, R. H.; Nielson, M. M.; Bechgaard, K.; Langeveld-Voss, B. M. W.; Spiering, A. J. H.; Janssen, R. A. J.; Meijer, E. W.; Herwig, P.; de Leeuw, D. M., *"Two-dimensional charge transport in self-organized, high-mobility conjugated polymers"*, Nature, **401**, 685-688, 1999**.**
(17) McCarthy, B.; Coleman, J. N.; Czerw, R.; Dalton, A. B.; Carroll, D. L.; Blau, W. J., *"Microscopy studies of nanotube-conjugated polymer interactions"*, Synth. Met., **121**, 1225-1226, 2001**.**
(18) McCarthy, B.; Coleman, J. N.; Czerw, R.; Dalton, A. B.; in het Panhuis, M.; Maiti, A.; Drury, A.; Bernier, P.; Nagy, J. B.; Lahr, B.; Byrne, H. J.; Carroll, D. L.; Blau, W. J., *"A Microscopic and Spectroscopic Study of Interactions between Carbon Nanotubes and a Conjugated Polymer"*, J. Phys. Chem. B., **106**, 2210-2216, 2002**.**
(19) Lei, S.-B.; Wan, L.-J.; Wang, C.; Bai, C.-L., *"Direct Observation of the Ordering and Molecular Folding of Poly[(m-phenylenevinylene)-co-(2,5-dioctoxy-p-phenylenevinylene)]"*, Adv. Mater., **16**, 828-831, 2004**.**
(20) Saito, R.; Dresselhaus, G.; Dresselhaus, M. S., *Physical Properties of Carbon Nanotubes*. Imperial College Press: London, 1998.
(21) Liu, J.; Rinzler, A. G.; Dai, H.; Hafner, J. H.; Bradley, R. K.; Boul, P. J.; Lu, A.; Iverson, T.; Shelimov, K.; Huffman, C. B.; Rodriguez-Macias, F.; Shon, Y.-S.; Lee, T. R.; Colbert, D. T.; Smalley, R. E., *"Fullerene Pipes"*, Science, **280**, 1253-1256, 1998**.**
(22) Raman, spectroscopy was used to establish the quality of treated single-walled carbon nanotube samples as well as the average nanotube diameter present using well established procedures (see reference 19).
(23) Ryan, K. P.; Lipson, S. M.; Drury, A.; Cadek, M.; Ruether, M.; O'Flaherty, S. M.; Barron, V.; McCarthy, B.; Byrne, H. J.; Blau, W. J.; Coleman, J. N., *"Carbon-nanotube nucleated crystallinity in a conjugated polymer based composite"*, Chem. Phys. Lett., **391**, 329-333, 2004**.**
(24) Mena-Osteritz, E.; Meyer, A.; Langeveld-Voss, B. M. W.; Janssen, R. A. J.; Meijer, E. W.; Bauerle, P., *"Two-Dimensional Crystals of Poly(3-Alkyl-thiophene)s: Direct Visualization of Polymer Folds in Submolecular Resolution"*, Angew. Chem. Int. Ed, **39**, 2680-2684, 2000**.**
(25) Sandberg, H. G. O.; Frey, G. L.; Shkunov, M. N.; Sirringhaus, H.; Friend, R. H.; Nielsen, M. M.; Kumpf, C., *"Ultrathin Regioregular Poly(3-hexyl thiophene) Field-Effect Transistors"*, Langmuir, **18**, 10176-10182, 2002**.**
(26) Prosa, T. J.; Winokur, M. J.; Moulton, J.; Smith, P.; Heeger, A. J., *"X-RAY STRUCTURAL STUDIES OF POLY(3-ALKYLTHIOPHENES) - AN EXAMPLE OF AN INVERSE COMB"*, Macromolecules, **25**, 4364-4372, 1992**.**
(27) Kymakis, E. PhD, University of Cambridge, 2003.
(28) in het Panhuis, M.; Maiti, A.; Dalton, A. B.; van den Noort, A.; Coleman, J. N.; McCarthy, B.; Blau, W. J., *"Selective interaction in a polymer-single-wall carbon nanotube composite"*, J. Phys. Chem. B., **107**, 478-482, 2003**.**
(29) Grévin, B.; Rannou, P.; Payerne, R.; Pron, A.; Travers, J. P., *"Multi-scale scanning tunneling microscopy imaging of self-organized regioregular poly(3-hexylthiophene) films"*, J. Chem. Phys., **118**, 7097-7102, 2003**.**
(30) Czerw, R.; Guo, Z.; Ajayan, P.; Sun, Y.; Carroll, D., *"Organisation of Polymers onto Carbon Nanotubes: A Route to Nanoscale Assembly"*, Nano Lett., **1**, 423-427, 2001**.**
(31) Economopoulos, S. P.; Govaris, G. K.; Chochos, C. L.; Tzanetos, N. P.; Andreaopoulou, A. K.; Kallitsis, J. K.; Yianoulis, P.; Gregoriou, V. G. In *Polymer Spectroscopy*, 15th European Symposium on Polymer Spectroscopy, Crete (Greece), 2003, Gregoriou, V. G., Ed. Wiley-VCH, 2004; pp 19-31.
(32) Cyr, D. M.; Venkataraman, B.; Flynn, G. W.; Black, A.; Whitesides, G. M., *"Functional Group Identification in Scanning Tunneling Microscopy of Molecular Adsorbates"*, Journal of Physical Chemistry, **100**, 13747-13759, 1996**.**
(33) Jackson, A. M.; Myerson, J. W.; Stellacci, F., *"Spontaneous assembly of subnanometre-ordered domains in the ligand shell of monolayer-protected nanoparticles"*, Nature Materials, **3**, 330 - 336, 2004**.**
(34) Coleman, J. N.; Ferreira, M. S., *"Geometric constraints in the growth of nanotube-templated polymer monolayers"*, Appl. Phys. Lett., **84**, 798-800, 2004**.**
(35) Wall, A.; Coleman, J. N.; Ferreira, M. S., *"Physical mechanism for the mechanical reinforcement in nanotube-polymer composite materials"*, Phys. Rev. B., **71**, 125421, 2005**.**
(36) Theander, M.; Yartsev, A.; Zigmantas, D.; Sundstrom, V.; Mammo, W.; Andersson, M. R.; Inganas, O., *"Photoluminescence quenching at a polythiophene/C60 heterojunction"*, Physical Review B: Condensed Matter and Materials Physics, **61**, 12957-12963, 2000**.**

(37) McCarthy, B.; Coleman, J. N.; Czerw, R.; Dalton, A. B.; Byrne, H. J.; Tekleab, D.; Iyer, P.; Ajayan, P. M.; Blau, W. J.; Carroll, D. L., *"Complex nano-assemblies of polymers and carbon nanotubes"*, Nanotechnology, **12**, 187-190, 2001**.**